Atmos. Chem. Phys. Discuss., 14, 21065–21099, 2014
www.atmos-chem-phys-discuss.net/14/21065/2014/
doi:10.5194/acpd-14-21065-2014


Atmospheric Chemistry and Physics Discussions
Open Access



# The influence of the North Atlantic Oscillation and El Niño–Southern Oscillation on mean and extreme values of column ozone over the United States

**I. Petropavlovskikh[1], R. Evans[2], G. McConville[1], G. L. Manney[3,4], and H. E. Rieder[5,6]**

[1]Cooperative Institute for Research in Environmental Sciences, University of Colorado, Boulder, CO 80309, USA
[2]NOAA Earth System Research Laboratory, Boulder, CO 80305, USA
[3]NorthWest Research Associates, Socorro, NM 87801, USA
[4]Department of Physics, New Mexico Institute of Mining and Technology, Socorro, NM 87801, USA
[5]Wegener Center for Climate and Global Change and IGAM/Institute of Physics, University of Graz, 8010 Graz, Austria
[6]Lamont-Doherty Earth Observatory of Columbia University, Palisades, NY 10964, USA

Received: 22 May 2014 – Accepted: 15 July 2014 – Published: 15 August 2014

Correspondence to: I. Petropavlovskikh (irina.petro@noaa.gov)

Published by Copernicus Publications on behalf of the European Geosciences Union.

## Abstract

Continuous measurements of total ozone (by Dobson spectrophotometers) across the contiguous United States (US) began in the early 1960s. Here, we analyze temporal and spatial variability and trends in total ozone from the five US sites with long-term records. While similar long-term ozone changes are detected at all five sites, we find differences in the patterns of ozone variability on shorter time scales. In addition to standard evaluation techniques, STL-decomposition methods (Seasonal Trend decomposition of time series based on LOcally wEighted Scatterplot Smoothing, LOESS) are used to address temporal variability and trends in the Dobson data. The LOESS-smoothed trend components show a decline of total ozone between the 1970s and 2000s and a "stabilization" at lower levels in recent years, which is also confirmed by linear trend analysis. Methods from statistical extreme value theory (EVT) are used to characterize days with high and low total ozone (termed EHOs and ELOs, respectively) at each station and to analyze temporal changes in the frequency of ozone extremes and their relationship to dynamical features such as the North Atlantic Oscillation and El Niño Southern Oscillation. A comparison of the "fingerprints" detected in the frequency distribution of the extremes with those for standard metrics (i.e., the mean) shows that more "fingerprints" are found for the extremes, particularly for the positive phase of the NAO, at all five US monitoring sites. Results from the STL-decomposition support the findings of the EVT analysis. Finally, we analyze the relative influence of low and high ozone events on seasonal mean column ozone at each station. The results show that the influence of ELOs and EHOs on seasonal mean column ozone can be as much as ±5 %, or about twice as large as the overall long-term decadal ozone trends.

## 1 Introduction

Long-term monitoring of ozone is critical because it is instrumental in controlling the levels of ultraviolet radiation reaching the planet's surface and thus plays an important





ACPD
14, 21065–21099, 2014

role in the existence of life on Earth (e.g., Tourpali et al., 2009; Bais et al., 2011; McKenzie et al., 2011). The 25th anniversary of the Montreal protocol (signed in 1987) marked an important milestone in the phasing out of man-made chemicals such as chlorofluorocarbons (CFCs), commonly referred to as ozone depleting substances (ODS). ODS have very long life times in the stratosphere (some as long as 100 years); they are lofted throughout the stratosphere from the tropical troposphere, transported into the middle and high latitudes, and recirculate, providing chlorine (and bromine) atoms for chemical ozone destruction (WMO, 2011; Rigby et al., 2013).

Analyses of inter-annual and long-term variability in total column ozone on regional (e.g., Mäder et al., 2007; Rieder et al., 2010a, b, 2011; Fitzka et al., 2014) and global (e.g., Frossard et al., 2013; Rieder et al., 2013) scales have been presented in a number of recent studies. There is now a broad consensus that long-term negative ozone trends are dominated by ODS, while short-term trends and variability, particularly at mid-latitudes, are also significantly influenced by synoptic-scale meteorological variability (e.g., Steinbrecht et al., 1998; Shepherd, 2008), decadal climate variability (e.g., Chandra et al., 1996; Hood, 1997) and dynamical modes such as the El Niño–Southern Oscillation (ENSO) (e.g., Brönnimann et al., 2004; Ziemke et al., 2010; Hood et al., 2010; Gabriel et al., 2011), the North Atlantic Oscillation (NAO)/Arctic Oscillation (AO) (e.g., Appenzeller et al., 2000; Thompson and Wallace, 2000) and volcanic eruptions (e.g., Jaeger and Wege, 1990; Solomon, 1999; Robock, 2000; Mäder et al., 2007). For the European Sector it has been reported that dynamical variability accounts for about a third of the observed ozone changes between the 1970s and 1990s (e.g., Mäder et al., 2007; Wohltmann et al., 2007). The particular importance of dynamical changes for column ozone at mid-latitudes has also been highlighted in more recent work that attributes the slight increase in column ozone since the 1990s primarily to dynamics and to a lesser extent to the decrease in ODS (after their peak around 1997) (e.g., Harris et al., 2008; Hegglin and Shepherd, 2009; WMO, 2007, 2011).

In addition, recent work analyzing the tails of the ozone distribution (i.e., the extremes) in relation to the bulk properties (i.e., the mean) showed that analysis of





ACPD
14, 21065–21099, 2014

the tails allows for a more systematic attribution of ozone changes to dynamical features than mean value analysis can achieve (e.g., Rieder et al., 2010a, b, 2011, 2013; Frossard et al., 2013). These studies also showed that even moderate NAO and ENSO events can have significant effects on the mid-latitude ozone field.

Furthermore, it has been noted that while column ozone at northern mid-latitudes reached its lowest values in the early 1990s, following the 1991 eruption of Mount Pinatubo, the effect of this eruption was partially masked by atmospheric dynamics in the Southern Hemisphere (e.g., Schnadt Poberaj et al., 2011; Rieder et al., 2013), again emphasizing the importance of atmospheric dynamics to ozone trends and variability.

In this paper we attempt to assess the information contained in the integrated total ozone column derived from the continental US network of Dobson measurements. We discuss interannual variability in ozone, how it has changed over the last 50 years, what controls it, and how trends are statistically related to dynamical and chemical proxies.

## 2 Data

### 2.1 Ground-based total ozone data sets

Continuous measurements of total column ozone (TOC) over the continental United States began in the early 1960s. Individual measurements were also made earlier at some sites, but more sporadically and mainly in conjunction with the International Geophysical Year 1957.

The backbone of the World Meteorological Organizations (WMO) ozone monitoring network is the Dobson Ozone Spectrophotometer, an instrument developed in the 1920s specifically for high accuracy measurements of total column ozone (e.g., Dobson, 1957, 1968). The concept of the Dobson measurement is the differential absorption of ozone at selected wavelengths in the solar ultraviolet spectrum. Two pairs, where one spectral range absorbs light more strongly than the other, are combined to min-





ACPD
14, 21065–21099, 2014

imize the effect of aerosol interference on the measurements. Measurements made using the direct solar beam are used to determine the TOC based on Lambert–Beers law, while measurements made with the scattered light from the zenith are converted to a TOC value based on the statistics of quasi-simultaneous measurements of both direct sun and zenith.

Operational instrument calibration is maintained by monthly tests with reference and discharge lamps, plus regular inter-comparison with two standard instruments: D083 (World Primary Standard) or D065 (World Secondary Standard). The calibration of the Primary Standard is maintained by Langley Plot Campaigns at the National Oceanic and Atmospheric Administration's Earth System Research Laboratory Mauna Loa Observatory (Hawaii).

In the contiguous US, column ozone has been measured routinely at five observational sites (Bismarck, ND; Boulder, CO; Caribou, ME; Wallops Island, VA; Nashville, TN) since the 1960s. In this study we analyze the total ozone records from these five sites spanning from the 1960s through 2012. A detailed overview on geographical location and information on record length, data completeness and time series properties of the individual station records is provided in Fig. 1.

### 2.2 Proxies for atmospheric dynamics

There is now a broad consensus that long-term trends in total ozone are driven primarily by changes in the atmospheric concentration of ozone depleting substances (ODS) (WMO, 2011). Nevertheless, active research in the field showed that besides ODS, several other processes have significant influence on total ozone changes and variability. The 11 year solar cycle, the Quasi-Biennial Oscillation (QBO) and volcanic eruptions are among the most prominent explanatory variables often used to describe the influence of atmospheric variability on column ozone (WMO, 2011). At mid-latitudes other dynamical features also show significant influence on column ozone on seasonal and inter-annual time scales. In particular, synoptic scale meteorological variability, described by, e.g., the North Atlantic Oscillation (NAO) (e.g., Appenzeller et al., 2000; Orsolini and Doblas-Reyes, 2003; Rieder et al., 2010b, 2011; Frossard et al., 2013), and climate modes such as El Niño–Southern Oscillation (ENSO) (e.g., Rieder et al., 2013, 2010b; Brönnimann et al., 2004) have been shown to significantly influence ozone variability and trends.

In the present study we focus particularly on the influence of atmospheric dynamics on variability and trends in column ozone over the US. To this aim we use a set of indices describing ENSO and NAO modes on seasonal basis in the statistical analysis. For ENSO we are using the seasonal NINO3.4 Index provided by NOAA's Climate Prediction Center – available at http://www.cpc.ncep.noaa.gov/data/indices/3mth.nino34.81-10.ascii.txt. For the NAO we are using the seasonal station-based index (based on the difference of normalized sea level pressures between Ponta Delgada, Azores and Stykkisholmur/Reykjavik, Iceland) provided by the NCAR/UCAR climate data center – available at https://climatedataguide.ucar.edu/sites/default/files/climate_index_files/nao_station_seasonal_1.txt.

# 3 Methods

## 3.1 Extreme value statistics

Recent work has introduced concepts of statistical extreme value theory (EVT) into the field of total ozone research (Rieder et al., 2010a, b, 2011, 2013; Frossard et al., 2013; Fitzka et al., 2014). Here we build on these methodologies to analyze extreme low and high ozone events (termed ELOs and EHOs, respectively), in the US long-term total ozone records.

The generalized Pareto distribution (GPD) is a commonly used distribution in the framework of extreme value theory (e.g., Davison and Smith, 1990; Ribatet et al., 2009) because it arises as the natural distribution for the exceedance of a random variable (here total ozone) over a threshold. Below we briefly describe the modeling procedure for values over a threshold. Note that the modeling for values below a threshold is





ACPD
14, 21065–21099, 2014

precisely the same, the only thing to be done is to negate the values and apply exactly the same procedure as for values above a high threshold as $\min(x_i) = -\max(-x_i)$.

The GPD, which is the limiting distribution of exceedances over a threshold, is defined as:

$$F(x) = 1 - \left[1 + \xi \frac{x-u}{\sigma}\right]^{-\frac{1}{\xi}}, \quad \sigma > 0, \quad x > u, \quad 1 + \xi \frac{x-u}{\sigma} > 0, \tag{1}$$

where $x$ are daily data (here total ozone), $u$ is the threshold value and $\sigma$ and $\xi$ are the scale (a measure of the spread of the distribution of $x$) and shape (which is determining the shape of the distribution rather than shifting it as $u$ does or shrinking/stretching it as $\sigma$ does) parameters, respectively.

Threshold values $u$ are determined on a monthly basis and interpolated to daily values following the procedure described by Rieder et al. (2010a). For convenient reference, thresholds for ELOs and EHOs, as well as long-term monthly mean values for the five US sites, are shown Fig. 2.

Following Rieder et al. (2010a) total ozone observations at the individual US sites are categorized in three groups (see Eqs. 2–4),

$$\mathrm{ELO} = \{x(t) : x(t) < u_{\mathrm{LOW}}(t)\}, \tag{2}$$

$$\mathrm{EHO} = \{x(t) : x(t) > u_{\mathrm{HIGH}}(t)\}, \tag{3}$$

$$\mathrm{NEO} = \{x(t) : u_{\mathrm{LOW}}(t) \le x(t) \le u_{\mathrm{HIGH}}(t)\}, \tag{4}$$

where, $x(t)$ is the column ozone amount at a given day, $u_{\mathrm{LOW}}(t)$ and $u_{\mathrm{HIGH}}(t)$ are the thresholds for low and high ozone on a given day, and ELO, EHO, NEO denote days with low, high, and non-extreme ozone, respectively. The frequency of low and high ozone events is discussed below in the context of dynamical features (see Sect. 4.1).

## 3.2 Seasonal Trend decomposition of time series based on LOESS (STL)

Seasonal Trend decomposition of the time series based on LOESS (LOcally wEighted Scatterplot Smoothing) (e.g., Cleveland et al., 1990) decomposes a data record (here ozone) into seasonality, trend and residual components. When applied to the US column ozone data it returns a well-known picture: (i) a strong seasonal cycle with maxima in spring and minima in winter/fall, in accordance with the understanding of the influence of the Brewer–Dobson circulation on column ozone (transport of ozone-rich air towards northern-mid-latitudes during boreal winter), (ii) a negative trend-component dominated by the influence of ODS on column ozone, and (iii) a highly variable residual component representing the effects of local scale meteorology on column ozone. An example of an STL-decomposition for the site in Boulder, CO is shown in Fig. S1 in the Supplement of this article. For a more detailed description of the STL-procedure we refer the interested reader to the paper of Cleveland et al. (1990) describing the method.

Our main interest in this study lies in the trend component of the STL-decomposition. Thus STL is applied to all 5 US Dobson records analyzed in this study. We utilize STL because the resulting trend component provides a more detailed picture of the seasonal and interannual variability in the overall time series compared to, e.g., a simple linear trend component.

## 4 Results

The main goal of this paper is to analyze the influence of dynamical features such as NAO and ENSO on column ozone over the US. To this aim EVT modeling and STL decomposition are applied to the long-term total ozone time series to derive "fingerprints" of the dynamical covariates.

### 4.1 "Fingerprints" of NAO and ENSO in the frequency distribution of extreme events

In Sect. 3.1 we described the classification of total ozone observations into days with extreme low, extreme high and non-extreme ozone. Here we focus on the frequency distribution of the extremes and analyze the influence of ENSO and NAO events on column ozone at the 5 US ozone monitoring sites. As the general features are very similar among the individual sites, we show mainly the results for Boulder and Caribou, which give the envelope of column ozone observations over the US, in the main body of the paper. For convenient reference, illustrations for other sites are available in the Supplement for this article. In Figs. 3 and 4 we plot the observed frequency of ELOs, NEOs and EHOs as time series for Boulder and Caribou (the results for the remaining sites are shown in Figs. S2–S4 in the Supplement). Next, we turn to "fingerprints" of atmospheric dynamics in the frequency distribution of EHOs and ELOs at these sites.

First, we turn to the North Atlantic Oscillation which is the leading mode in the Atlantic sector, influencing the direction and intensity of the tropospheric jet stream (e.g., Orsolini and Limpasuvan, 2001) and representing the main driver of the inter-annual variability in storm tracks during the cold season (e.g., Lau, 1988). A positive NAO phase leads to lower ozone over Europe and the US and higher ozone over Labrador and Greenland, and vice versa for a negative NAO phase (see Rieder et al., 2010b and references therein; and Frossard et al., 2013 for a spatial representation of NAO influence on column ozone at northern mid-latitudes).

The North Atlantic Oscillation in its negative phase (NAO index $< -1$, marked with blue (winter) and light blue (spring) dots in Figs. 3 and 4) leads to higher column ozone over the United States during winter and spring. Conversely, a "fingerprint" of the NAO in its positive phase (NAO index $> 1$, marked with red (winter) and orange (spring) dots in Figs. 3 and 4) is seen as lower ozone over the US in the individual station records. Over the study period (1963–2012), the NAO has been in a strongly positive phase (NAO index $> 1$) 16 times during winter and 12 times during spring. While all but one of the wintertime events are captured in the frequency of ELOs at multiple sites, 2 out of the 12 spring events remain undetected (1982 and 1994) at any of the five US sites (see Fig. 6).

It has been noted that the NAO has tended towards a more positive phase in recent decades (e.g., Hurrel, 1995; Thompson and Wallace, 2000), concomitant with





ACPD
14, 21065–21099, 2014

a strengthening of the northern polar vortex. Nevertheless, a strongly negative NAO phase (NAO index < −1) is found 10 times during winter and 5 times during spring (roughly half the rate of positive phase events) in 1963–2012. Out of the 10 wintertime events 8 are discernible in the frequency distribution of extreme total ozone, with the winters of 1973/74 and 2010/11 being absent. The missing NAO "fingerprint" in winter 2010/11 is not surprising given the unusual dynamical conditions in the Arctic in this year, which led to a particularly strong stratospheric polar vortex and record Arctic ozone losses (e.g., Manney et al., 2011), counteracting the dynamic enhancement of column ozone due to the NAO. Out of the 5 springtime negative NAO events, 3 can be identified in (most of) the 5 US monitoring sites, with 2005 and 2006 missing. As was the case in 2011, the particularly cold conditions in the Arctic spring of 2005 likely contribute to the missing NAO "fingerprint".

The NAO "fingerprints" identified in the US column ozone records are in broad agreement with those for European sites and satellite data (e.g., Frossard et al., 2013; Rieder et al., 2011), confirming the significant influence of the NAO on column ozone variability throughout northern mid-latitudes.

Next we turn to the El Niño–Southern Oscillation. Warm ENSO events are triggered by a high contrast between tropical and extratropical Pacific sea-surface temperatures, which are known to affect mid-latitudes (in particular the North Pacific) via changes in the Hadley cell and Rossby wave generation (e.g., Trenberth, 1998; Alexander et al., 2002). During warm ENSO events, the meridional circulation in the stratosphere leads to enhanced ozone transport from the tropics to middle and high latitudes and a warmer lower stratosphere, both of which tend to increase mid-latitude ozone (Rieder et al., 2013, and references therein).

The warm ENSO phase (El Niño, NINO3.4 index > 0.7) is, as expected, associated with higher ozone over the US during winter/spring, visible in the frequency distribution of the extremes. During the study period, moderate to strongly positive ENSO events have been recorded 11 times during winter and 4 times during spring. Most wintertime events (except those in 1983, 1992 and 1995) and springtime events (except 1983 and





ACPD
14, 21065–21099, 2014

1992) can be identified in the frequency distribution of ozone extremes. The absence of ENSO "fingerprints" in the remaining 3 years is consistent with their occurrence immediately after the two major volcanic eruptions of the last century (El Chichon in 1982 and Mt. Pinatubo in 1991), when the effects of the volcanic eruptions (enhanced ozone depletion on sulfate aerosols) would have masked the dynamical signal. As was the case for the NAO, the ENSO results for the US sites are in good agreement with findings for European sites and satellite data (e.g., Rieder et al., 2010b, 2013), illustrating the importance of ENSO in modulating column ozone at northern mid-latitudes.

At all sites we find a more consistent presence of fingerprints of NAO and ENSO in extreme values of column ozone (upper panels in Figs. 3 and 4) than in its mean values (lower panels of Figs. 3 and 4). While the extremes show a pronounced response (increasing or decreasing frequency) to the prevailing ENSO and NAO phases, the mean values often do not show large differences compared to neighboring years without ENSO or NAO events. This is particularly evident for NAO+ events, where about twice as many events were detected in the frequency distribution of the extremes than in the seasonal mean values.

### 4.2 "Fingerprints" of atmospheric dynamics in the STL decomposition

Here we contrast the findings of the EVT-based analysis with results from the STL-decomposition approach. In Fig. 5 we show the anomaly of the trend components of the STL-decomposition for the two selected US sites, Boulder and Caribou, as above in the EVT-analysis (the results for the remaining sites are shown in Fig. S5 in the Supplement). While the overall trend curves show a steady decline that is most pronounced in the 1980s and 1990s, as expected from the strong negative influence of ODS on column ozone (e.g., WMO, 2011), there is also a large degree of inter-annual variability in these curves. This variability is not related to seasonality in the ozone field, since the seasonal component has been removed from the data prior to the trend calculations with the STL-procedure.





ACPD

14, 21065–21099, 2014

As for the EVT-analysis we now identify "fingerprints" of ENSO and NAO events in the STL trend component. The colored vertical bars in Fig. 5a and c mark positive and negative winter- and spring time NAO events. The analysis of the STL trend-component shows that positive NAO events are associated with a decreasing tendency in the trend curve, and thus with lower column ozone, while negative NAO events are associated with an increasing tendency in the STL trend component, and thus with higher column ozone. Figure 5b and d shows the corresponding results for warm ENSO events, which tend to enhance column ozone.

The good agreement between the results in Fig. 5 with those from the EVT-analysis (Figs. 3 and 4) provides further evidence for the significant influence of strong NAO and ENSO events on column ozone variability over the continental US.

The STL trend-decomposition anomalies also show that the strong negative tendencies present during the 1980s and 1990s came to halt around the turn of the century. In recent years the trend components at all sites shows a high degree of interannual variability, though with an overall stabilization at lower column ozone levels. This result suggests that although there is as yet no definitive sign of ozone recovery in the US column ozone records, the period of pronounced ozone loss is seen to have come to halt, a feature that has also been seen in other ground based sites and in results from state-of-the-art chemistry climate model calculations (e.g., SPARC-CCMVal, 2010; Eyring et al., 2010). We will evaluate this qualitative finding in more detail in Sect. 4.4.

### 4.3 Similarities and differences among the individual monitoring sites

Despite the overall similarity in trends and patterns of variability, it is important to note that "fingerprints" of individual NAO and ENSO events are not always found at all 5 stations analyzed. Figure 6 provides a summary of all major ENSO and NAO events over the 1963–2012 time period and their detection (or absence) in the individual station records. Solid squares in Fig. 6 mark "fingerprints" detected while open squares mark "absent" fingerprints at individual sites. The majority of ENSO and NAO events are detected at all 5 US total ozone monitoring sites, but some individual events are





ACPD
14, 21065–21099, 2014

not discernible at individual (or multiple) sites such as, e.g., the negative NAO event of spring 1996. The absence of individual "fingerprints" is not too surprising given the large spatial distance among individual sites (see Fig. 1) and is attributed to regional effects such as masking by synoptic-scale meteorology (e.g., the influence of the subtropical jets and localized tropopause variations) and regional patterns of advection and convergence or divergence related to changes in tropospheric and stratospheric pressure systems, which exert local influences on column ozone, as has been previously reported for other regions (e.g., Koch et al., 2005; Mäder et al., 2007; Wohltmann et al., 2007). The absence of individual "fingerprints" on site basis and their underlying cause is of general interest, though beyond the spatial and climatological scope of the presented study. Nevertheless further analysis (including also vertical information from sounding profiles) is suggested for future site specific analysis addressing effects of local dynamics on column ozone variability.

### 4.4 Influence of extreme events on ozone mean values and trends

In this section we turn the focus to column ozone trends at the five US Dobson sites. To analyze the influence of extremes (both low and high) on ozone trends we contrast linear trends for the entire observational time series (i.e., all observational data included) with trends for time series with extremes removed. We focus on two main time periods: (1) 1970–2000, the period with almost linearly increasing ODSs and thus largest ozone depletion, and (2) the period from 1990–2010, which spans the peak in ozone depletion (Mt. Pinatubo) and maximum ODSs ($\sim$ 2000) to current conditions. Results for each site during winter and spring are given in Tables 1 and 2.

During the period with almost linearly increasing ODS (1970–2000; Table 1) ozone trends vary between −2 and −3.5 % per decade among the sites and seasons. All sites except Caribou show larger negative trends in spring than in winter, consistent with results from European mid-latitude sites (e.g., Rieder et al., 2010b, 2011). We argue that this qualitative difference between Caribou and the other US sites is determined by geography. Caribou is the northernmost US monitoring site and thus is more fre-





ACPD
14, 21065–21099, 2014

quently affected by transport of air masses out of the Arctic polar regions in winter and spring than the other stations; such Arctic air may, in particularly cold winters, carry the signature of chemical ozone depletion. The more southerly sites are usually most strongly influenced by mid-latitude ozone-rich air masses (e.g., Manney et al., 2014), though they may also show effects of transport of low-ozone air from low latitudes and accompanying troposphere to stratosphere exchange.

Comparing the entire observational records with those with extremes removed, we find that trends are only about half as strong in the latter case. This is particularly interesting as neither EHOs nor ELOs show statistically significant trends in their magnitude over 1970–2000. The individual time series show the well-known pattern of large interannual variability but no robust increase (or decrease) in the average magnitude of the extremes themselves. Thus the influence of extremes on seasonal mean column ozone (see below) can be understood as a function of their occurrence frequency, driven by chemical ozone depletion and dynamics.

Turning now to the more recent past, i.e., the last two decades (Table 2), we find positive trends at all sites, an unsurprising result since the period with largest mid-latitude ozone losses in the early 1990s has been followed by a period of slowly but steadily declining ODS. The key interest in the trends for 1990–2010 is thus not the sign of the trends but their significance. Observational and modelling studies suggest that chemical ozone depletion ceased to increase around the turn of the century (e.g., WMO, 2011), but whether significant ozone recovery has started is still undetermined. The positive signs in Table 2 indicate that ozone has stopped declining over the US, suggesting that chemical depletion may have ceased. Nevertheless, since the trend estimates over the 20 year period 1990–2010 typically do not exceed the standard errors (given in parentheses in Table 2), there is no clear evidence that significant ozone recovery has started yet. As was the case for 1970–2000, the trends are much smaller (a factor of 2–3) if extremes are removed from the records. Again we investigate whether significant changes occurred in the extremity of ELOs and EHOs and, as for the 1970–2000 period, we find large interannual variability in the magnitude of lows





ACPD
14, 21065–21099, 2014

and highs (driven by dynamics and chemistry) though no significant trends at rigorous test levels (i.e., 95 %).

Discriminating the effects of the individual dynamical proxies on column ozone is difficult because: (i) "fingerprints" for multiple proxies are found in several years (e.g., a strongly positive NAO and a warm ENSO phase) and (ii) the occurrence frequency of the individual "fingerprints" is highly variable. Instead, we quantify the overall contribution of extremes to seasonal mean column ozone by calculating the influence of ELOs and EHOs at each site:

$$I_{\mathrm{ELOs}} = \left(\frac{M_{\mathrm{s}} - M_{\mathrm{sELO(ex)}}}{M_{\mathrm{s}}}\right) \cdot 100 \tag{5}$$

$$I_{\mathrm{EHOs}} = \left(\frac{M_{\mathrm{s}} - M_{\mathrm{sEHO(ex)}}}{M_{\mathrm{s}}}\right) \cdot 100 \tag{6}$$

where $I_{\mathrm{ELOs}}$ ($I_{\mathrm{EHOs}}$) is the influence of extreme low (high) total ozone on seasonal mean column ozone ($M_{\mathrm{s}}$) in percent, and $M_{\mathrm{sELO(ex)}}$ ($M_{\mathrm{sEHO(ex)}}$) is the seasonally averaged column ozone with ELOs (EHOs) excluded from the time series. In Figs. 7 and 8 we show the influence of ELOs and EHOs on winter and spring column ozone, respectively. While EHOs are the dominant influence in the early and late parts of the station records, the time period from 1980–2000 is dominated by the influence of ELOs, consistent with the nearly linear increase in ODSs and their importance to column ozone changes in this time period. During this period of strong ozone depletion, however, individual years still show a net positive effect of the extremes on seasonal mean column ozone, highlighting the importance of dynamical factors, such as warm ENSO events (e.g., spring 1986 and 1998), on column ozone variability. The influence of ELOs and EHOs on seasonal mean ozone is bound by about ±5 % , thus can be about twice as large as the overall long-term trend values given in Table 1.

Next we analyze the pattern correlation of the net contribution of the extremes (i.e., $I_{\mathrm{ELOs}} + I_{\mathrm{EHOs}}$) among individual sites. The seasonal pattern correlations among individual sites are summarized in Table 3. Pattern correlations are highest for neighboring sites, i.e., Boulder-Bismarck and Nashville-Wallops Island. Caribou is again an exception in this respect, with a seasonally dependent correlation with the other sites. During winter, the correlation at Caribou is highest with the eastern sites (Nashville and Wallops Island), while during spring, the correlation is highest with the western sites (Bismarck and Boulder), suggesting that Caribou is under the influence of the same air masses as the eastern/western sites during different seasons. Examinations of the overall correlations for each decade of the record (not shown here) indicates that the correlation between Boulder and Nashville (particularly in winter) increases with time (i.e., it is higher in the 1990s and 2000s than in the 1970s and 1980s), while the correlation between Nashville and Wallops Island slightly decreased in recent decades (in both winter and spring), consistent with Boulder and Nashville being more frequently influenced by similar air masses in recent years. Recent operational changes at Caribou, resulting in reduced sampling frequency, significantly affect the correlation between Caribou and Wallops Island, thus highlighting the importance of continuous and frequent ozone observations for both trend analysis and assessment of relationships between measurements at different sites.

## 5 Discussion and conclusions

In this study we analyze data from the five long-term Dobson stations across the contiguous US to investigate the influence of the Northern Atlantic Oscillation (NAO) and the El Niño–Southern Oscillation (ENSO) on total ozone variability and trends since the 1960s. In addition to standard evaluation techniques we utilize a STL-decomposition method (Seasonal-Trend decomposition procedure based on LOESS) and statistical extreme value theory (EVT) to address the temporal variability and trends in the Dobson data in relation to synoptic-scale meteorological and climate variability.

The results show that "fingerprints" of the dynamical features are better captured in the tails (i.e., the extremes) than in the bulk (i.e., the mean) of the observational





ACPD
14, 21065–21099, 2014

records, a result in broad agreement with earlier work for European monitoring sites (Rieder et al., 2010b, 2011) and satellite data (e.g., Frossard et al., 2013; Rieder et al., 2013). "Fingerprints" of individual ENSO and NAO events are coherently captured at a majority of the sites, indicating the large-scale influence of these features on column ozone. The observed increase in the frequency of ELOs and decrease in the frequency of EHOs from the 1970s on is in agreement with the notion of increasing ODS and the expansion of the tropical band and the contraction of the northern polar band (e.g., Hudson et al., 2006; Seidel et al., 2008). During the 1980–2000 period, when ozone depletion was strongest, individual years still show a net positive contribution of the extremes to seasonal mean column ozone, demonstrating the importance of individual negative NAO and warm ENSO events for ozone variability.

In agreement with earlier work we find significant negative trends in column ozone over the US in 1970–2000 (the period with almost linearly increasing ODS). Although column ozone values over the US ceased to decrease around the turn of the century, the observational records for 1990–2010 generally show positive, but insignificant, trends, and thus do not yet show a clear signature of the onset of ozone recovery. Trends derived excluding extremes from the records are much smaller than those derived from the full records, consistent with previous results for other regions and datasets. The contribution of low and high ozone events to winter and spring mean column ozone is bound by about ±5 %, a value about twice as large as the mean negative trends in 1970–2000, indicating the importance of dynamics to ozone variability and trends.

Pattern correlations of the contribution of low and high ozone events to seasonal mean column ozone are highest for neighboring sites (i.e., Bismarck-Boulder and Nashville-Wallops Island), though not homogenous among sites (e.g., seasonally dependent and time varying among individual sites). Trends for individual sub-periods (i.e., 1980–2000 and 1990–2010) are of the same sign at all sites, but differ in magnitude and significance among seasons and time periods analyzed.





ACPD
14, 21065–21099, 2014

The results presented here highlight the importance of a continued spatially-distributed long-term ozone monitoring program to address future ozone changes and to detect and confirm the onset and progress of ozone recovery in the context of the Montreal Protocol.

**The Supplement related to this article is available online at doi:10.5194/acpd-14-21065-2014-supplement.**

*Acknowledgements.* The authors wish to express appreciation to the NOAA Weather Service personnel whose efforts in making the Dobson ozone measurements over sixty years allow us to study some of the longest atmospheric constituent time series in existence. The authors thank the NOAA Climate Prediction Center and NCAR/UCAR climate data center for providing ENSO and NAO Indices used in this study via their respective data portals.

## References

Alexander, M. J., Tsuda, T., and Vincent, R. A.: Latitudinal variations observed in gravity waves with short vertical wavelengths, J. Atmos. Sci., 59, 1394–1404, 2002.

Appenzeller, C., Weiss, A. K., and Staehelin, J.: North Atlantic oscillation modulates total ozone winter trends, Geophys. Res. Lett., 27, 1131–1134, 2000.

Bais, A. F., Tourpali, K., Kazantzidis, A., Akiyoshi, H., Bekki, S., Braesicke, P., Chipperfield, M. P., Dameris, M., Eyring, V., Garny, H., Iachetti, D., Jöckel, P., Kubin, A., Langematz, U., Mancini, E., Michou, M., Morgenstern, O., Nakamura, T., Newman, P. A., Pitari, G., Plummer, D. A., Rozanov, E., Shepherd, T. G., Shibata, K., Tian, W., and Yamashita, Y.: Projections of UV radiation changes in the 21st century: impact of ozone recovery and cloud effects, Atmos. Chem. Phys., 11, 7533–7545, doi:10.5194/acp-11-7533-2011, 2011.

Brönnimann, S., Luterbacher, J., Staehelin, J., Svendby, T. M., Hansen, G., and Svenoe, T.: Extreme climate of the global troposphere and stratosphere in 1940–42 related to El Nino, Nature, 431, 971–974, doi:10.1038/nature02982, 2004.

Chandra, S., Varotsos, C., and Flynn, L. E.: The mid-latitude total ozone trends in the Northern Hemisphere, Geophys. Res. Lett., 23, 555–558, 1996.
Cleveland, R. B., Cleveland, W. S., McRae, J. A., and Terpenning, I.: STL: a Seasonal-Trend decomposition procedure based on LOESS, Journal of Official Statistics, 6, 3–73, 1990.
Davison, A. C. and Smith, R. L.: Models for exceedances over high thresholds (with Discussion), J. Roy. Stat. Soc. B, 52, 393–442, 1990.
Dobson, G. M. B.: Observers' handbook for the ozone spectrophotometer, Ann. Int. Geophys. Year, 5, 46–89, 1957.
Dobson, G. M. B.: 40 years research on atmospheric ozone at Oxford – a history, Appl. Optics, 7, 387–405, doi:10.1364/Ao.7.000387, 1968.
Eyring, V., Cionni, I., Bodeker, G. E., Charlton-Perez, A. J., Kinnison, D. E., Scinocca, J. F., Waugh, D. W., Akiyoshi, H., Bekki, S., Chipperfield, M. P., Dameris, M., Dhomse, S., Frith, S. M., Garny, H., Gettelman, A., Kubin, A., Langematz, U., Mancini, E., Marchand, M., Nakamura, T., Oman, L. D., Pawson, S., Pitari, G., Plummer, D. A., Rozanov, E., Shepherd, T. G., Shibata, K., Tian, W., Braesicke, P., Hardiman, S. C., Lamarque, J. F., Morgenstern, O., Pyle, J. A., Smale, D., and Yamashita, Y.: Multi-model assessment of stratospheric ozone return dates and ozone recovery in CCMVal-2 models, Atmos. Chem. Phys., 10, 9451–9472, doi:10.5194/acp-10-9451-2010, 2010.
Fitzka, M., Hadzimustafic, J., and Simic, S.: Total ozone and Umkehr observations at Hoher Sonnblick 1994–2011: climatology and extreme events, J. Geophys. Res., 119, 739–752, doi:10.1002/2013JD021173, 2014.
Frossard, L., Rieder, H. E., Ribatet, M., Staehelin, J., Maeder, J. A., Di Rocco, S., Davison, A. C., and Peter, T.: On the relationship between total ozone and atmospheric dynamics and chemistry at mid-latitudes – Part 1: Statistical models and spatial fingerprints of atmospheric dynamics and chemistry, Atmos. Chem. Phys., 13, 147–164, doi:10.5194/acp-13-147-2013, 2013.
Gabriel, A., Körnich, H., Lossow, S., Peters, D. H. W., Urban, J., and Murtagh, D.: Zonal asymmetries in middle atmospheric ozone and water vapour derived from Odin satellite data 2001–2010, Atmos. Chem. Phys., 11, 9865–9885, doi:10.5194/acp-11-9865-2011, 2011.
Harris, N. R. P., Kyrö, E., Staehelin, J., Brunner, D., Andersen, S.-B., Godin-Beekmann, S., Dhomse, S., Hadjinicolaou, P., Hansen, G., Isaksen, I., Jrrar, A., Karpetchko, A., Kivi, R., Knudsen, B., Krizan, P., Lastovicka, J., Maeder, J., Orsolini, Y., Pyle, J. A., Rex, M., Vanicek, K., Weber, M., Wohltmann, I., Zanis, P., and Zerefos, C.: Ozone trends at north-





ACPD
14, 21065–21099, 2014

ern mid- and high latitudes – a European perspective, Ann. Geophys., 26, 1207–1220, doi:10.5194/angeo-26-1207-2008, 2008.
Hegglin, M. I. and Shepherd, T. G.: Large climate-induced changes in ultraviolet index and stratosphere-to-troposphere ozone flux, Nat. Geosci., 2, 687–691, doi:10.1038/ngeo604, 2009.
Hood, L. L.: The solar cycle variation of total ozone: dynamical forcing in the lower stratosphere, J. Geophys. Res.-Atmos., 102, 1355–1370, 1997.
Hood, L. L., Soukharev, B. E., and McCormack, J. P.: Decadal variability of the tropical stratosphere: secondary influence of the El Niño–Southern Oscillation, J. Geophys. Res.-Atmos., 115, D11113, doi:10.1029/2009jd012291, 2010.
Hudson, R. D., Andrade, M. F., Follette, M. B., and Frolov, A. D.: The total ozone field separated into meteorological regimes – Part II: Northern Hemisphere mid-latitude total ozone trends, Atmos. Chem. Phys., 6, 5183–5191, doi:10.5194/acp-6-5183-2006, 2006.
Jaeger, H. and Wege, K.: Stratospheric ozone depletion at northern mid-latitudes after major volcanic eruptions, J. Atmos. Chem., 10, 273–287, 1990.
Koch, G., Wernli, H., Schwierz, C., Staehelin, J., and Peter, T.: A composite study on the structure and formation of ozone miniholes and minihighs over central Europe, Geophys. Res. Lett., 32, L12810, doi:10.1029/2004gl022062, 2005.
Lau, N. C.: Variability of the observed midlatitude storm tracks in relation to low-frequency changes in the circulation pattern, J. Atmos. Sci., 45, 2718–2743, 1988.
Mäder, J. A., Staehelin, J., Brunner, D., Stahel, W. A., Wohltmann, I., and Peter, T.: Statistical modeling of total ozone: selection of appropriate explanatory variables, J. Geophys. Res.-Atmos., 112, D11108, doi:10.1029/2006jd007694, 2007.
Manney, G. L., Santee, M. L., Rex, M., Livesey, N. J., Pitts, M. C., Veefkind, P., Nash, E. R., Wohltmann, I., Lehmann, R., Froidevaux, L., Poole, L. R., Schoeberl, M. R., Haffner, D. P., Davies, J., Dorokhov, V., Gernandt, H., Johnson, B., Kivi, R., Kyro, E., Larsen, N., Levelt, P. F., Makshtas, A., McElroy, C. T., Nakajima, H., Parrondo, M. C., Tarasick, D. W., von der Gathen, P., Walker, K. A., and Zinoviev, N. S.: Unprecedented Arctic ozone loss in 2011, Nature, 478, 469–475, doi:10.1038/nature10556, 2011.
Manney, G. L., Hegglin, M. I., Daffer, W. H., Schwartz, M. J., and Santee, M. L.: Climatology of Upper Tropospheric-Lower Stratospheric (UTLS) jets and tropopauses in MERRA, J. Climate, 27, 3248–3271, doi:10.1175/JCLI-D-13-00243.1, 2014.





ACPD
14, 21065–21099, 2014

The influence of the NAO and ENSO on mean and extreme values of column ozone over the US

I. Petropavlovskikh et al.

Title Page
Abstract | Introduction
Conclusions | References
Tables | Figures
◀| |▶
◀ ▶
Back | Close
Full Screen / Esc
Printer-friendly Version
Interactive Discussion

McKenzie, R. L., Aucamp, P. J., Bais, A. F., Bjorn, L. O., Ilyas, M., and Madronich, S.: Ozone depletion and climate change: impacts on UV radiation, Photochem. Photobio. S., 10, 182–198, doi:10.1039/C0pp90034f, 2011.

Orsolini, Y. J. and Doblas-Reyes, F. J.: Ozone signatures of climate patterns over the Euro-Atlantic sector in the spring, Q. J. Roy. Meteor. Soc., 129, 3251–3263, doi:10.1256/qj.02.165, 2003.

Orsolini, Y. J. and Limpasuvan, V.: The North Atlantic Oscillation and the occurrences of ozone miniholes, Geophys. Res. Lett., 28, 4099–4102, 2001.

Ribatet, M., Ouarda, T., Sauquet, E., and Gresillon, J. M.: Modeling all exceedances above a threshold using an extremal dependence structure: inferences on several flood characteristics, Water Resour. Res., 45, W03407, doi:10.1029/2007wr006322, 2009.

Rieder, H. E., Staehelin, J., Maeder, J. A., Peter, T., Ribatet, M., Davison, A. C., Stübi, R., Weihs, P., and Holawe, F.: Extreme events in total ozone over Arosa – Part 1: Application of extreme value theory, Atmos. Chem. Phys., 10, 10021–10031, doi:10.5194/acp-10-10021-2010, 2010a.

Rieder, H. E., Staehelin, J., Maeder, J. A., Peter, T., Ribatet, M., Davison, A. C., Stübi, R., Weihs, P., and Holawe, F.: Extreme events in total ozone over Arosa – Part 2: Fingerprints of atmospheric dynamics and chemistry and effects on mean values and long-term changes, Atmos. Chem. Phys., 10, 10033–10045, doi:10.5194/acp-10-10033-2010, 2010b.

Rieder, H. E., Jancso, L. M., Di Rocco, S., Staehelin, J., Maeder, J. A., Peter, T., Ribatet, M., Davison, A. C., De Backer, H., Koehler, U., Krzyscin, J., and Vanicek, K.: Extreme events in total ozone over the Northern mid-latitudes: an analysis based on long-term data sets from five European ground-based stations, Tellus B, 63, 860–874, doi:10.1111/j.1600-0889.2011.00575.x, 2011.

Rieder, H. E., Frossard, L., Ribatet, M., Staehelin, J., Maeder, J. A., Di Rocco, S., Davison, A. C., Peter, T., Weihs, P., and Holawe, F.: On the relationship between total ozone and atmospheric dynamics and chemistry at mid-latitudes – Part 2: The effects of the El Niño/Southern Oscillation, volcanic eruptions and contributions of atmospheric dynamics and chemistry to long-term total ozone changes, Atmos. Chem. Phys., 13, 165–179, doi:10.5194/acp-13-165-2013, 2013.

Rigby, M., Prinn, R. G., O'Doherty, S., Montzka, S. A., McCulloch, A., Harth, C. M., Mühle, J., Salameh, P. K., Weiss, R. F., Young, D., Simmonds, P. G., Hall, B. D., Dutton, G. S., Nance, D., Mondeel, D. J., Elkins, J. W., Krummel, P. B., Steele, L. P., and Fraser, P. J.: Re-evaluation of the lifetimes of the major CFCs and $CH_3CCl_3$ using atmospheric trends, Atmos. Chem. Phys., 13, 2691–2702, doi:10.5194/acp-13-2691-2013, 2013.

Robock, A.: Volcanic eruptions and climate, Rev. Geophys., 38, 191–219, 2000.

Schnadt Poberaj, C., Staehelin, J., and Brunner, D.: Missing stratospheric ozone decrease at Southern Hemisphere middle latitudes after Mt. Pinatubo: a dynamical perspective, J. Atmos. Sci., 68, 1922–1945, 2011.

Seidel, D. J., Fu, Q., Randel, W. J., and Reichler, T. J.: Widening of the tropical belt in a changing climate, Nat. Geosci., 1, 21–24, doi:10.1038/ngeo.2007.38, 2008.

Shepherd, T. G.: Dynamics, stratospheric ozone, and climate change, Atmos. Ocean, 46, 117–138, doi:10.3137/ao.460106, 2008.

Solomon, S.: Stratospheric ozone depletion: a review of concepts and history, Rev. Geophys., 37, 275–316, 1999.

SPARC CCMVal: SPARC Report on the Evaluation of Chemistry-Climate Models, edited by: Eyring, V., Shepherd, T. G., Waugh, D. W., SPARC Report No. 5, WCRP-132, WMO/TD-No. 1526, 2010.

Steinbrecht, W., Claude, H., Kohler, U., and Hoinka, K. P.: Correlations between tropopause height and total ozone: implications for long-term changes, J. Geophys. Res.-Atmos., 103, 19183–19192, 1998.

Thompson, D. W. J. and Wallace, J. M.: Annular modes in the extratropical circulation. Part I: Month-to-month variability, J. Climate, 13, 1000–1016, 2000.

Tourpali, K., Bais, A. F., Kazantzidis, A., Zerefos, C. S., Akiyoshi, H., Austin, J., Brühl, C., Butchart, N., Chipperfield, M. P., Dameris, M., Deushi, M., Eyring, V., Giorgetta, M. A., Kinnison, D. E., Mancini, E., Marsh, D. R., Nagashima, T., Pitari, G., Plummer, D. A., Rozanov, E., Shibata, K., and Tian, W.: Clear sky UV simulations for the 21st century based on ozone and temperature projections from Chemistry-Climate Models, Atmos. Chem. Phys., 9, 1165–1172, doi:10.5194/acp-9-1165-2009, 2009.

Trenberth, K. E.: Progress during TOGA in understanding and modeling global teleconnections associated with tropical sea surface temperatures, J. Geophys. Res., 103, 14291–14324, 1998.

WMO: Scientific Assessment of Ozone Depletion: 2006, Global Ozone Research and Montitoring Project 50, Geneva, Switzerland, 572, 2007.

WMO: Scientific Assessment of Ozone Depletion: 2010, Global Ozone Research and Montitoring Project 50, Geneva, Switzerland, 516, 2011.





ACPD
14, 21065–21099, 2014

Wohltmann, I., Lehmann, R., Rex, M., Brunner, D., and Mader, J. A.: A process-oriented regression model for column ozone, J. Geophys. Res.-Atmos., 112, D12304, doi:10.1029/2006jd007573, 2007.
Ziemke, J. R., Chandra, S., Oman, L. D., and Bhartia, P. K.: A new ENSO index derived from satellite measurements of column ozone, Atmos. Chem. Phys., 10, 3711–3721, doi:10.5194/acp-10-3711-2010, 2010.





ACPD
14, 21065–21099, 2014

The influence of the NAO and ENSO on mean and extreme values of column ozone over the US

I. Petropavlovskikh et al.

Title Page
Abstract | Introduction
Conclusions | References
Tables | Figures
◀I | ▶I
◀ | ▶
Back | Close
Full Screen / Esc
Printer-friendly Version
Interactive Discussion

**Table 1.** Seasonal linear trends (in % decade$^{-1}$) for observed and extremes removed winter (DJF) and spring (MAM) column ozone time series in 1970–2000 at the 5 US ozone monitoring sites. Standard errors are given in parentheses.

| | trend (in % decade$^{-1}$) for 1970–2000 | |
|---|---|---|
| season/station | observations | no extremes |
| DJF | | |
| Bismarck | −2.2 (±0.6) | −0.8 (±0.3) |
| Boulder | −1.7(±0.6) | −0.5 (±0.4) |
| Caribou | −3.2 (±0.8) | −1.0 (±0.5) |
| Wallops Island | −2.4 (±0.8) | −1.0 (±0.5) |
| Nashville | −2.2 (±0.7) | −1.0 (±0.4) |
| MAM | | |
| Bismarck | −3.6 (±0.6) | −1.6 (±0.4) |
| Boulder | −3.5 (±0.7) | −1.9 (±0.4) |
| Caribou | −2.3 (±0.8) | −1.0 (±0.4) |
| Wallops Island | −2.7 (±0,7) | −1.3 (±0.5) |
| Nashville | −3.5 (±0.8) | −1.9 (±0.4) |





ACPD
14, 21065–21099, 2014

**Table 2.** As Table 1 but for 1990–2010.

| | trend (in % $decade^{-1}$) for 1990–2010 | |
|---|---|---|
| season/station | observations | no extremes |
| DJF | | |
| Bismarck | 2.2 (±1.3) | 1.5 (±0.7) |
| Boulder | 1.1 (±1.4) | 0.3 (±0.8) |
| Caribou | 2.4 (±1.5) | 1.2 (±1.2) |
| Wallops Island | 3.1 (±1.5) | 1.6 (±0.9) |
| Nashville | 1.3 (±1.4) | 0.4 (±0.7) |
| MAM | | |
| Bismarck | 2.0 (±1.1) | 1.2 (±0.8) |
| Boulder | 0.9 (±1.4) | 0.7 (±0.7) |
| Caribou | 1.0 (±1.1) | 0.1 (±0.8) |
| Wallops Island | 1.1 (±1.3) | 0.9 (±0.9) |
| Nashville | 1.0 (±1.3) | 0.5 (±0.7) |





ACPD
14, 21065–21099, 2014

The influence of the NAO and ENSO on mean and extreme values of column ozone over the US

I. Petropavlovskikh et al.

**Table 3.** Pattern correlation of the net influence of extremes on winter (DJF) and spring (MAM) mean column ozone among the 5 US ozone monitoring sites. For station code see Fig. 1.

| Season/Stations | | | | | |
|---|---|---|---|---|---|
| | BIS | BDR | CAR | WAI | BNA |
| DJF | | | | | |
| BIS | – | 0.64 | 0.48 | 0.42 | 0.6 |
| BDR | 0.64 | – | 0.51 | 0.34 | 0.58 |
| CAR | 0.48 | 0.51 | – | 0.69 | 0.63 |
| WAI | 0.42 | 0.34 | 0.69 | – | 0.69 |
| BNA | 0.6 | 0.58 | 0.63 | 0.69 | – |
| MAM | | | | | |
| BIS | – | 0.76 | 0.69 | 0.59 | 0.6 |
| BDR | 0.76 | – | 0.61 | 0.68 | 0.65 |
| CAR | 0.69 | 0.61 | – | 0.5 | 0.52 |
| WAI | 0.59 | 0.68 | 0.5 | – | 0.72 |
| BNA | 0.6 | 0.65 | 0.52 | 0.72 | – |





ACPD
14, 21065–21099, 2014

The influence of the NAO and ENSO on mean and extreme values of column ozone over the US

I. Petropavlovskikh et al.

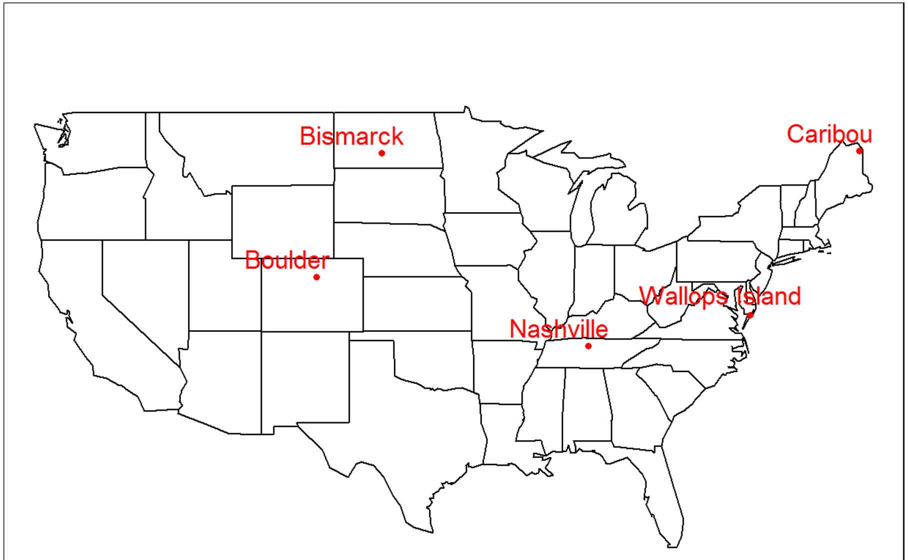


| STATION | SITE ID | LATITUDE | LONGITUDE | RECORD STARTS | # observations | MEAN TOC | MAX/MIN TOC |
|---|---|---|---|---|---|---|---|
| Bismarck,ND | BIS | 46.8°N | 100.8°W | Dec 1962 | 15669 | 330 | 531/221 |
| Boulder,CO | BDR | 40.0°N | 105.3°W | Sep 1967 | 10980 | 309 | 492/218 |
| Caribou,ME | CAR | 46.9°N | 68.0°W | Aug 1962 | 11587 | 348 | 626/210 |
| Wallops Island, VA | WAI | 37.9°N | 75.5°W | Jun 1968 | 9082 | 318 | 522/217 |
| Nashville, TN | BNA | 36.2°N | 86.6°W | Jul 1962 | 14581 | 310 | 504/213 |

**Figure 1.** Geographical overview and site specific information for the US long-term Dobson total ozone monitoring sites.





ACPD
14, 21065–21099, 2014

The influence of the NAO and ENSO on mean and extreme values of column ozone over the US

I. Petropavlovskikh et al.

Title Page
Abstract | Introduction
Conclusions | References
Tables | Figures
◀| |▶
◀ ▶
Back | Close
Full Screen / Esc
Printer-friendly Version
Interactive Discussion

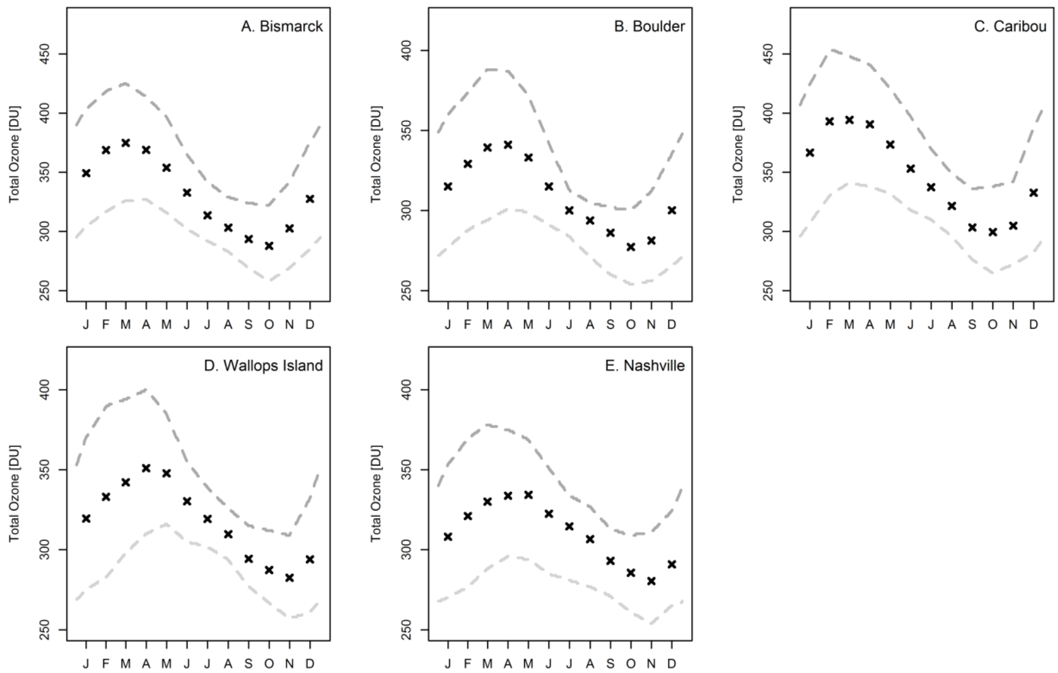


**Figure 2.** Thresholds for extreme highs (EHOs, dark grey dashed lines) and lows (ELOs, light grey dashed lines) of total ozone and climatological monthly means of total ozone (black crosses) at **(A)** Bismarck, **(B)** Boulder, **(C)** Caribou, **(D)** Wallops Island and **(E)** Nashville.

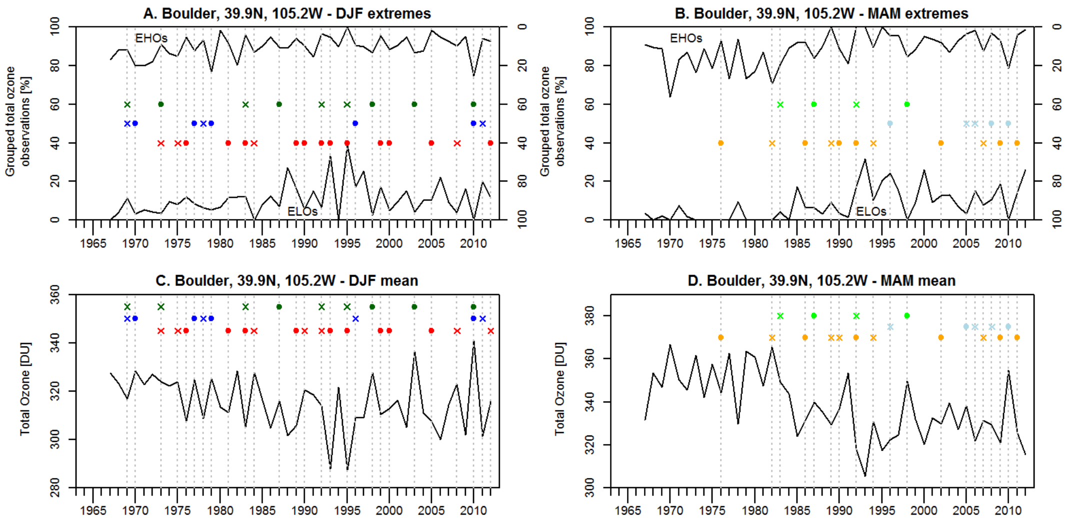


**Figure 3.** "Fingerprints" of the NAO and ENSO as detected for Boulder in **(A)** the frequency distribution of EHOs and ELOs for winter (DJF), **(B)** as **(A)** but for spring (MAM), **(C)** as **(A)** but for "fingerprints" in seasonal mean column ozone, **(D)** as **(C)** but for spring. Filled circles denote visible "fingerprints" and crosses denote not visible "fingerprints". NAO positive (negative) phase is indicated for winter in red (blue) and for spring in orange (light blue), ENSO positive phase is indicated for winter (spring) in green (light green).





ACPD
14, 21065–21099, 2014

The influence of the NAO and ENSO on mean and extreme values of column ozone over the US

I. Petropavlovskikh et al.

Title Page
Abstract | Introduction
Conclusions | References
Tables | Figures
◀| |▶
◀ ▶
Back | Close
Full Screen / Esc
Printer-friendly Version
Interactive Discussion

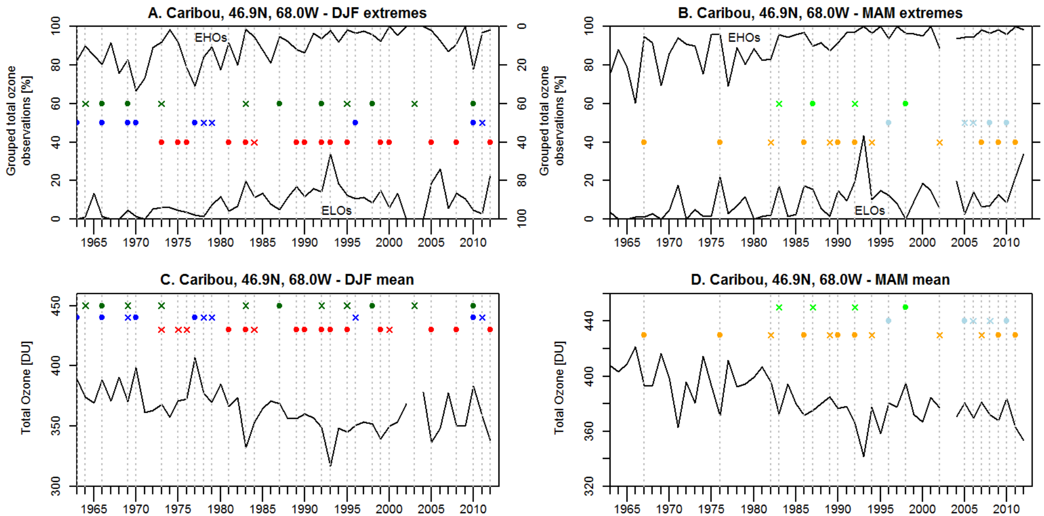


**Figure 4.** As Fig. 3 but for Caribou.





ACPD
14, 21065–21099, 2014

The influence of the NAO and ENSO on mean and extreme values of column ozone over the US

I. Petropavlovskikh et al.

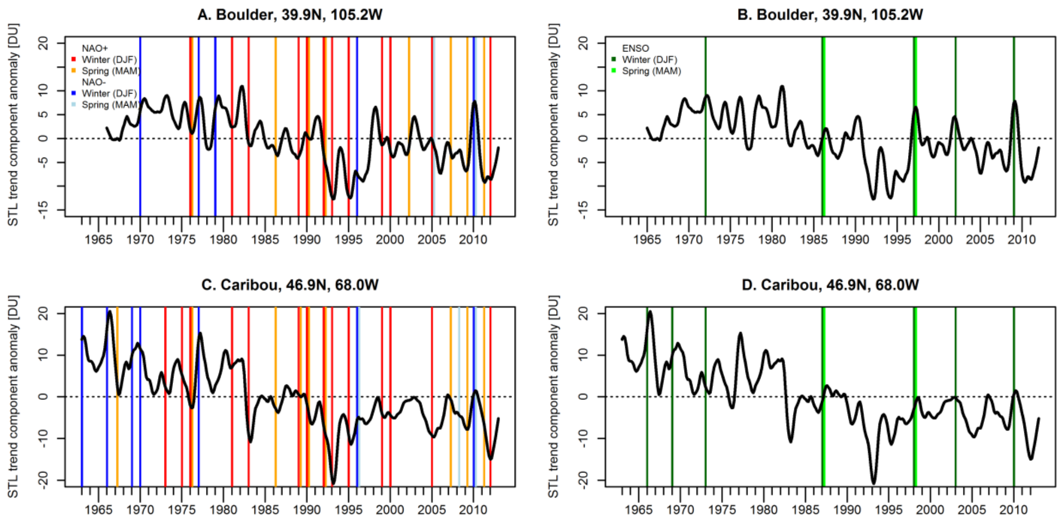


**Figure 5.** STL-trend component anomaly (in DU) in 1963–2012 for Boulder (top) and Caribou (bottom) with underlying marks (colored vertical bars) for "fingerprints" of positive and negative NAO modes (left panels) and warm ENSO phases (right panels) on seasonal basis. NAO positive (negative) phase is indicated for winter in red (blue) and for spring in orange (light blue). Warm ENSO phase is indicated for winter in green and spring in light green.





ACPD
14, 21065–21099, 2014

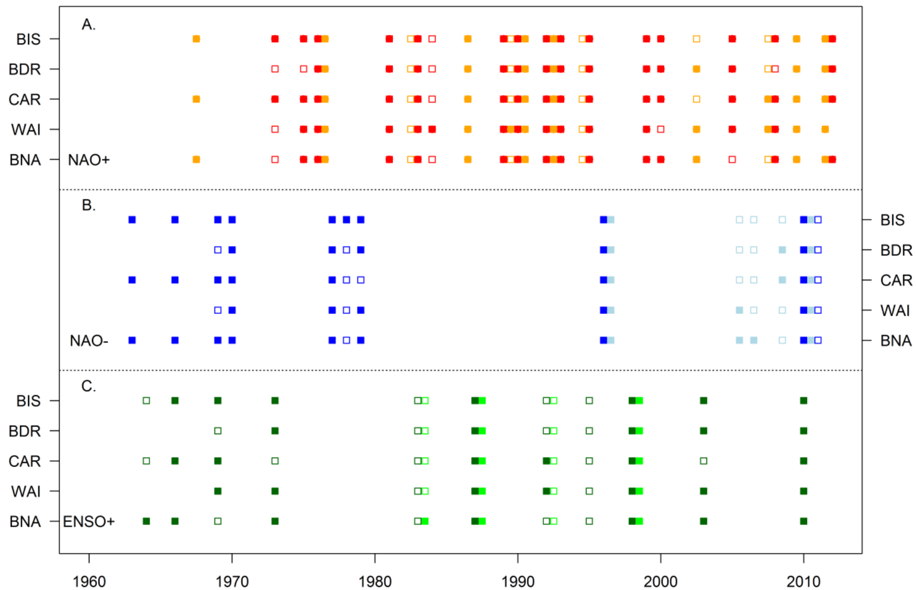


**Figure 6.** Summary of detected and missed "fingerprints" at all 5 US stations for **(A)** the NAO in its positive phase (winter red, spring orange), **(B)** the NAO in its negative phase (winter blue, spring light blue), and **(C)** ENSO in its warm phase (winter green, spring light green). Filled squares mark visible "fingerprints" while open squares mark not visible "fingerprints".





ACPD
14, 21065–21099, 2014

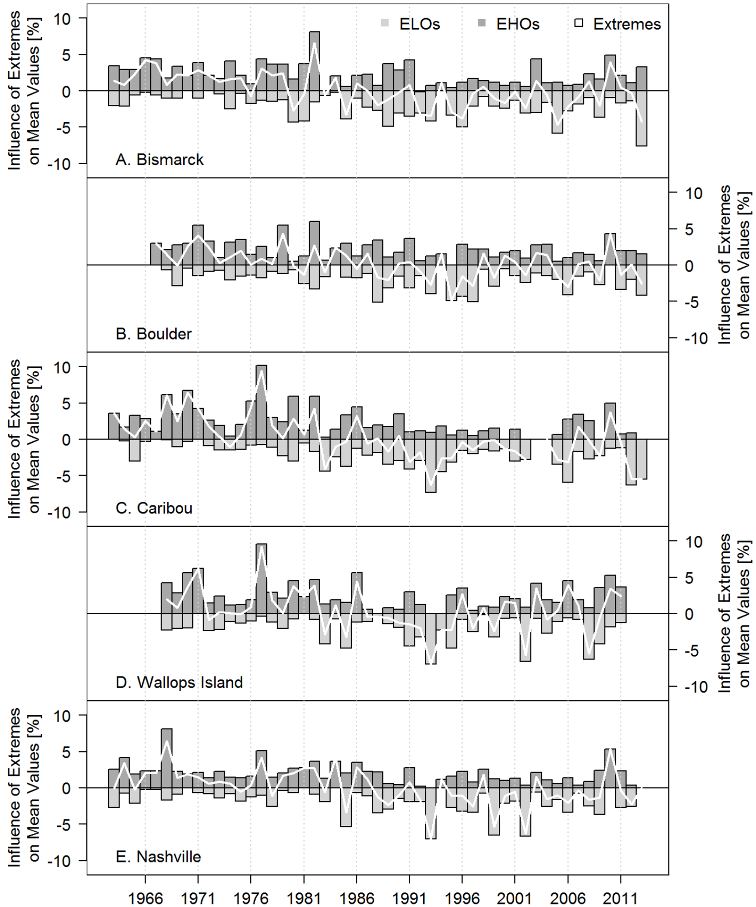


**Figure 7.** Influence (in %) of extreme low (ELOs, light histogram) and high (EHOs, dark histogram) ozone events and net influence of extremes (white curve) on winter (DJF) mean ozone at **(A)** Bismarck, **(B)** Boulder, **(C)** Caribou, **(D)** Wallops Island, and **(E)** Nashville.

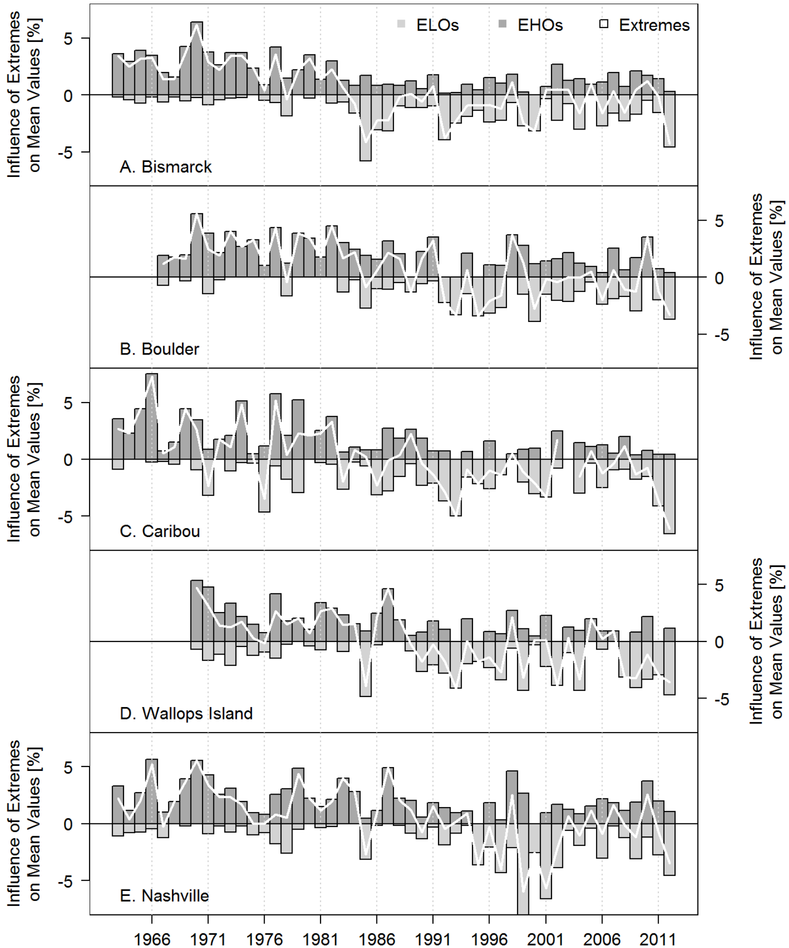


**Figure 8.** As Fig. 7 but for spring (MAM).





ACPD
14, 21065–21099, 2014

The influence of the NAO and ENSO on mean and extreme values of column ozone over the US

I. Petropavlovskikh et al.

Title Page
Abstract | Introduction
Conclusions | References
Tables | Figures
Back | Close
Full Screen / Esc
Printer-friendly Version
Interactive Discussion